DOI:
10.1038/ncb3532

Document Version
Other version

Supplementary Figure Legends

Supplementary Figure 1 | K14ΔNLef1 phenotypes, Gata6 expression in wild type adult skin. Gata6-tdTomato reporter analysis and Gata6 ChIP-Seq a, Late K14ΔNLef1 phenotypes: ectopic sebaceous glands (SG) (middle panel) and cysts (right panel). Haematoxylin and Eosin stained dorsal skin sections from wild type (WT) and K14ΔNLef1 mice at 22 weeks. **b**, Heatmap of genes that are differentially expressed between WT and K14ΔNLef1 epidermal cells. **c**, RT-qPCR of RNA from microdissected WT and K14ΔNLef1 hair follicles (HF) compared to heart (positive control for Gata4 and Gata6 expression). Data are means ± s.d. from three independent biological samples. **d**, Tamoxifen treated (lower panel) and untreated (top panel) Lgr6EGFPCreERT2 Rosa26-fl/STOP/fl-tdTomato back skin sections stained with antibodies to Gata6. **e,** Adult WT dorsal skin sections (bottom panels) or tail epidermal whole mounts (top panels) were stained for Gata6 and markers for different hair follicle stem cell populations. (d, e) Insets are higher magnification views of boxed areas. **f**, Adult ear skin sections from Gata6 reporter mouse showing co-localization of endogenous Gata6 and tdTomato. **g, h,** Gata6-tdTomato adult ear (g) and tail (h) epidermal whole mounts showing endogenous tdTomato and Krt14 antibody labelling. White arrows indicate the absence of Gata6 expression in lower growing HF during anagen. Yellow brackets indicate the bulge areas. **i,** A Z stack image (left panel) of a HF from whole mount tail Gata6-tdTomato epidermis stained with anti-Krt14. Orthogonal images from the 3D reconstruction (right panels), at the plane indicated by the white lines, show basal cell Gata6 expression confined to the junctional zone in proximity to the sebaceous glands (upper right panel). Flow cytometry analysis of Gata6-tdTomato dorsal epidermis shows absence of Gata6+CD34+ cells in adult telogen HF (right panel). **j**, Gata6 and Gapdh western blot of control (empty vector) and Gata6-overexpressing cultured primary mouse keratinocytes. **k**, Average signal intensity of Gata6 binding sites detected by two Gata6 antibodies (blue and light blue). **l**. Representative plots of ChIP-Seq reads aligned to the Lpl and Cldn4 gene loci. **m**, Motif enrichment analysis on Gata6 target regions performed by Meme Suite identified Gata6 expected DNA consensus and putative co-regulators. Scale bars: 50 μm; 150 μm.

Supplementary Figure 2 | Structural complexity of the junctional zone (JZ) revealed by gene expression profiling and antibody labelling. **a**, Expression profile analysis (RT–qPCR) of sorted basal JZ cells (green), non-basal SD cells (violet), bulge cells (yellow) and all remaining basal cells (grey) from telogen mouse back skin. Data are means ± s.d. N≥3 mice. **b, c** Gata6 and Blimp1 co-localize in the outermost differentiated layers of the JZ/SD. Wild type tail epidermal section stained for Gata6 and Blimp1 (b, top panels). Masks after color threshold analysis with ImageJ software and single fluorescent channel images of the magnified white insert are shown (b, bottom panels). Quantification of Gata6 expression in Blimp1 positive cells in JZ/SD and IFE (c). N=35 images from 4 mice. Data are means ± s.e.m. **d-j**, Wild type back (d, f, g) or tail (e, h, i, j) skin sections stained with the indicated antibodies. Dashed lines demarcate epidermal-dermal boundaries. Scale bars: 50 μm.

Supplementary Figure 3 | Additional data confirming the role of Gata6 in specifying the SD lineage. a, RT-qPCR of mRNA from dorsal epidermis of wild type (WT) and Gata6 knockout (cKO) mice confirming loss of Gata6 expression in the Gata6 cKO. **b**, Quantification of basal Itga6+Cd34- keratinocytes by flow cytometry (see Fig. 1h). **c**, Tail skin sections from WT, Gata6 epidermal knockout (cKO), K14ΔNLef1 and K14ΔNLef1 x Gata6 cKO (K14ΔNLef1 cKO) stained for the duct marker Plet1. Inserts are higher magnification views. **d, e,** K14ΔNLEF1 cysts express Plet1 and Atp6v1c2 and expression is reduced in the absence of Gata6. RT–qPCR analysis of mRNA from WT, cKO, K14ΔNLef1 and K14ΔNLef1 cKO epidermis (d). K14ΔNLef1 and K14ΔNLef1 cKO back skin sections were stained for the SD marker Atp6v1c2 and the SG marker Scd1 (e). Data are means ± s.d. from 3 to 5 mice. *P<0.05; **P<0.005. Scale bars: 50 μm. f, Gene Ontology enrichment analysis of Gata6 direct target genes highly expressed in Gata6+Itga6+ cells (see Fig. 2a). **g**, Plots of ChIP-Seq reads aligned to the Cep55, Ncaph and Spc24 (representative genes involved in mitosis) loci are shown. **h**, RT–qPCR of RNA from wild type (WT), Gata6 knockout (cKO), K14ΔNLef1 and K14ΔNLef1 x Gata6 cKO (K14ΔNLef1 cKO) epidermal cells. **i-k,** Validation of gene expression profiles from manual microdissected tail interfollicular epidermis (IFE), hair follicles (HF)

and sebaceous glands (SG). Bright field image of tail epidermal whole mount showing schematic of microdissection strategy (i). Z score heat maps representing array results for differentially expressed genes (j) validated by RT-qPCR (k). Data are means ± s.d. from 3 to 4 mice. EPID = Whole tail epidermis **l**, Sections of wild type (WT), Gata6 epidermal knockout (cKO), K14ΔNLef1 and K14ΔNLef1 x Gata6 cKO (K14ΔNLef1 cKO) dorsal skin stained for Gata6 and Blimp1 showing reduction in Blimp1+ cells in HF but not IFE in absence of Gata6. Inserts are higher magnification views of the JZ (red channel only). Asterisk indicates nonspecific staining. Dashed lines indicate epidermal-dermal boundary. Scale bar: 50 μm. **m,** Nuclear Androgen Receptor, Ar (black arrows), normally present in WT SG (insert panel), is reduced in K14 Δ NLef1 ectopic SG (top panel) but restored in K14 Δ NLef1 epidermis when Gata6 is ablated (bottom panel). Back skin sections were labeled with Ar antibody. **o**, RT–qPCR analysis of RNA from WT, cKO, K14ΔNLef1 and K14ΔNLef1 cKO adult back skin dermis. Data are means ± s.d. from 3 to 5 mice. *P<0.05. **p**, Schematic representation of Gata6 regulation of Ar and Blimp1. Scale bars: 50 μm.

Supplementary Figure 4 | Gata6 genetic labeling of epidermis under homeostatic conditions and Gata6 regulation by Vitamin A and Myc. **a**, Untreated (top left panel) and tamoxifen (4OHT) treated adult back skin sections from Gata6EGFPCreERT2 x Rosa26-fl/STOP/fl-tdTomato reporter mice. Dotted white lines indicate sebaceous glands. Samples were collected at the time points indicated. Gata6 genetically labeled cells are restricted to the junctional zone and sebaceous ducts (white arrow) and are not present in the lower HF. Scale bars: 25 μm. **b**, Schematic of known upstream regulators of Gata6 expression in multiple cell contexts[11, 12]. **c,** The transcription factor Myc induces Gata6 expression in the junctional zone, in the sebaceous glands and in the interfollicular epidermis (white arrows); in contrast, in K14 Δ NLef1 skin, Gata6 expression is only induced in the interfollicular epidermal cysts (see Fig. 1c). Sections of tamoxifen treated dorsal skin from wild type (WT) and K14MycER mice[10] stained for Gata6 (red) and Krt14 (green). **d, e,** Quantification of Gata6 expressing cells per hair follicle (d) and per length of interfollicular epidermis (IFE) (e) in the indicated mouse strains. Box-and-whisker plots: mid-line, median; box, 25th to 75th percentiles; and whiskers,

minimum and maximum. (N=12). **f, g,** Gata6 expression in the interfollicular epidermis correlates with the presence of ectopic SG (white and black arrowheads) in Tamoxifen treated skin from K14MycER mice. Dorsal skin sections were stained with Haematoxylin and Eosin (f) or Gata6 and Scd1 (g). **h, i**, Treatment with Vitamin A (Retinoid Acid – RA) leads to the presence of Gata6 expressing suprabasal cells in the interfollicular epidermis and lower hair follicle (white arrows) of adult dorsal skin, where normally Gata6 is not expressed. Acetone- (vehicle) and RA-treated skin sections were stained for Gata6, Ki67, and Fabp5. Insert with white lines is magnified in right panel (h). Dashed lines demarcate epidermal-dermal boundaries. Scale bars: 50 μm.

Supplementary Figure 5 | Characterization and quantification of Lrig1 and Gata6 genetically labelled (GL) cells prior to wounding and during re-epithelialization a, Quantification of Gata6 and Lrig1 genetically labeled (GL) cells after tamoxifen treatment, 48 hours after wounding in tail skin (N=5 mice, 116 HF for Gata6; 27 HF for Lrig1). Data are means ± s.d. **b**, Flow cytometry analysis showing lack of EdU incorporation by GL Gata6 tail keratinocytes in unwounded skin. Representative flow cytometry plots of epidermal Lrig1 (dark grey) and Gata6 (red) GL cells from back and tail skin (top left panels)**.** Gates in upper panels mark EdU positive cells analyzed in bottom left density plots (dashed yellow lines demarcate tdTomato negative controls). Quantification of EdU incorporation in all epidermal cells (top right panels) and tdTomato Gata6 (red) or Lrig1 (dark grey) GL cells (bottom right panels) is shown. (N=6 mice for Gata6; N=3 mice for Lrig1). Data are means ± s.d. **c**, Histological analysis confirming the absence of EdU incorporation into GL Gata6 in unwounded tail skin. Tail skin sections showing tdTomato GL Gata6 (left) or Lrig1 cells (right)) and EdU localization. EdU masks after color threshold analysis with ImageJ software together with tdTomato mask (top panel) or single tdTomato channel (bottom panel) are shown. Quantification of EdU incorporation by GL (Lrgi1 or Gata6) cells in JZ/SD (N=3 mice each; 49HF) is shown. Scale bars: 50 μm **d**, Suprabasal Gata6 GL cells acquire a basement membrane position during wound re-epithelialisation. Position in the epidermal layers of Gata6 GL cells at the indicated day after wounding tail skin is shown. Measurements are position relative to the basement

membrane of the lowest Gata6 GL cell of a column of labelled cells in the wound bed ("0" corresponds to the basal cell layer). 3-4 mice (average of 70 columnar cell units per mouse). The yellow bars in the violin plots represent median and black lines the 25th and 75th percentiles. **e**, Quantification of flow cytometry analysis of High-Itga6 and Mid/Low-Itga6 expressing Gata6 and Lrig1 GL cells in the tail wound bed at the indicated days after wounding. Data are means ± s.d. from 3 to 4 mice. Representative flow cytometric plots (right panels) are shown. Light blue lines represent gating strategy used for quantification in left hand panel[13]. *P<0.05; **P<0.005. **f**, Quantification of Ki67+ Lrig1 and Gata6 tdTomato GL cells at day 6 after wounding. Data are means ± s.e.m. from 25 cell clusters.

Supplementary Figure 6 | Fate of Blimp1 genetically labelled cells during wound healing. a, Blimp1-eGfp reporter mouse shows Blimp1 promoter activity in differentiated epidermal layers in undamaged epidermis and in the wound bed. Section of re-epithelialised wound from Blimp1-eGfp mouse stained for Gfp (green) and Itga6 (red). White arrow indicates newly formed dermal condensate in the magnified insert (Gfp channel only). **b**, **c,** Sections of back skin showing Blimp1 genetically labelled cells (green) in Blimp1Cre cag-cat-eGfp mice stained for Itga6 (red) in homeostatic (b) and hyperproliferative (c) skin. Hyperproliferation was induced by irradiation with 1000 J/m^2 UVB. White arrows indicate eGfp labelled Blimp1 expressing cells in the differentiated epidermal layers. **d**, Section of re-epithelialized wounded back skin stained with antibodies to Blimp1 and Krt14. Blimp1 expression is restricted to terminally differentiated epidermal cells in undamaged epidermis and in the wound bed. Inserts with white lines are higher magnification views. Scale bar: 50 μm. **e,** Differentiated, Blimp1 positive, epidermal cells dedifferentiate during re-epithelialization. Section of back skin showing Blimp1 lineage cells (red) stained with Itga6. White arrows (left hand insert) indicate tdTomato expressing Blimp1 GL cells in the differentiated epidermal layers far from the wound area. In the middle insert tdTomato labeled Blimp1 cells in the dermal papilla are shown. Right insert shows wound edge. The yellow boxed area is further magnified in the right hand panels. Single fluorescent channel images (left to right: dapi, Itga6, tdTomato) of two Gata6 GL cells indicated by the yellow arrows are shown. **f-h,**

Sections of tail (f, g) or back skin (h) at the indicated time points after wounding showing columns of IFE cells derived from dedifferentiation of Blimp1 GL cells (tdTomato). Sections are stained with Krt14 or Itga6. Nuclear expression of Blimp1 (red) is restricted to the suprabasal layers in the wound bed (g, lower panel). Representative images from 3 mice per time point. Inserts with white lines are higher magnification views. Dashed lines indicate dermal-epidermal junction. ND = not detected. Scale bars: 50 μm; 25 μm .

Supplementary Figure 7 | Additional evidence for the plasticity of differentiated Gata6+ cells following skin reconstitution. Epidermal cells isolated from the back skin of Gata6-tdTomato reporter/GFP-expressing adult mice in telogen were sorted into differentiated Gata6 Itga6 low/ tdTomato positive and Itga6 high cells. These two populations were compared in a skin reconstitution assay (Fig. 6). **a**, **b**. Graft skin sections stained for Gfp (green) and Krt14 (red). Single fluorescent channel images (a) and magnification of boxed inserts (b, left panels) are shown. Yellow arrows indicate Gfp positive basal cells derived from Gata6+ Itga6 low cells in the sebaceous gland (a). Dashed lines demarcate epidermal-dermal boundaries. Scale bars: 25 μm.

Supplementary Figure 8 | Time lapse imaging of migration of suprabasal Gata6 GL cells during wound healing in adult ear skin. a, A single stack image at 0 hour indicating the wound edge (magenta dotted line), HFs (white dotted circles), nuclei and collagen (green) and Gata6 genetically labeled (GL) cells (red). The thickness used to reconstruct the orthogonal images to be able to follow the entire group of Gata6 GL cells over time shown in Fig. 7a is indicated by the yellow rectangle. Scale bars: 100 μm. **b**, Quantification of the speed of cell migration according to whether cells moved upward, downward or straight. **c**, **d**, Representative examples of straight (c) and upward (d) migration of Gata6 GL cells (white arrows) are shown. Orthogonal images at the indicated time points from the beginning of image acquisition showing tdTomato labeled cells (red), nuclei and collagen (green). White lines indicate the basal membrane. Cartoons summarising the cell movements are shown in the top left panels. **e, f** Cell shape and size analysis of Gata6 GL cells during wound healing. Snapshots from live

imaging during wound healing (Fig. 7) were analyzed to assess size and shape of Gata6 GL cells that attached to the basement membrane compared to Gata6 GL cells that maintained a suprabasal position and unlabelled keratinocytes. Heat-mapped XY-view of the shapes of suprabasal Gata6 GL cells (left panel, N=18) and Gata6 GL cells that attached to the basement membrane (BM) (right panel, N=9) (e). Individual cells were aligned to the same XY centroid position and rotated to align wound direction horizontally to the right. Note that newly BM-attached GL cells were elongated toward the axis of wound direction as quantified in (f) (Right panel). Quantification of Gata6 GL cell size with reference to control keratinocytes in mouse ear skin (f). The reference cell size was obtained by in vivo labelling of keratinocytes by injection of Isolectin into WT mouse ear skin. Note that Gata6 GL cell that newly attached to the basement membrane had a similar size to normal basal keratinocytes (left panel). Quantification of cell elongation toward the axis of wound direction through the quantification of the migration shape index (MSI), defined as the ratio (α/β) of cell length projected to the axis of wound direction (α) over cell length perpendicular to the axis (β). Blue dotted line indicates MSI = 1, no elongation) (right panel). Data are means ± s.d. *P<0.05; **P<0.005.

Supplementary Movie 1 3D representation of Gata6 positive cells in the JZ/SD visualised with the Gata6-tdTomato reporter. Confocal Z stack projections of tail epidermal whole mount rendered using Volocity software.

1. Page, M.E., Lombard, P., Ng, F., Gottgens, B. & Jensen, K.B. The epidermis comprises autonomous compartments maintained by distinct stem cell populations. *Cell stem cell* **13**, 471-482 (2013).
2. Snippert, H.J., Haegebarth, A., Kasper, M., Jaks, V., van Es, J.H., Barker, N., van de Wetering, M., van den Born, M., Begthel, H., Vries, R.G., Stange, D.E., Toftgard, R. & Clevers, H. Lgr6 marks stem cells in the hair follicle that generate all cell lineages of the skin. *Science* **327**, 1385-1389 (2010).
3. Nguyen, H., Rendl, M. & Fuchs, E. Tcf3 governs stem cell features and represses cell fate determination in skin. *Cell* **127**, 171-183 (2006).
4. Nowak, J.A., Polak, L., Pasolli, H.A. & Fuchs, E. Hair follicle stem cells are specified and function in early skin morphogenesis. *Cell stem cell* **3**, 33-43 (2008).
5. Veniaminova, N.A., Vagnozzi, A.N., Kopinke, D., Do, T.T., Murtaugh, L.C., Maillard, I., Dlugosz, A.A., Reiter, J.F. & Wong, S.Y. Keratin 79 identifies a novel population of migratory epithelial cells that initiates hair canal morphogenesis and regeneration. *Development* **140**, 4870-4880 (2013).

6. Joost, S., Zeisel, A., Jacob, T., Sun, X., La Manno, G., Lonnerberg, P., Linnarsson, S. & Kasper, M. Single-Cell Transcriptomics Reveals that Differentiation and Spatial Signatures Shape Epidermal and Hair Follicle Heterogeneity. *Cell systems* **3**, 221-237 e229 (2016).
7. Collins, C.A. & Watt, F.M. Dynamic regulation of retinoic acid-binding proteins in developing, adult and neoplastic skin reveals roles for beta-catenin and Notch signalling. *Developmental biology* **324**, 55-67 (2008).
8. Horsley, V., O'Carroll, D., Tooze, R., Ohinata, Y., Saitou, M., Obukhanych, T., Nussenzweig, M., Tarakhovsky, A. & Fuchs, E. Blimp1 defines a progenitor population that governs cellular input to the sebaceous gland. *Cell* **126**, 597-609 (2006).
9. Kretzschmar, K., Cottle, D.L., Donati, G., Chiang, M.F., Quist, S.R., Gollnick, H.P., Natsuga, K., Lin, K.I. & Watt, F.M. BLIMP1 is required for postnatal epidermal homeostasis but does not define a sebaceous gland progenitor under steady-state conditions. *Stem cell reports* **3**, 620-633 (2014).
10. Cottle, D.L., Kretzschmar, K., Schweiger, P.J., Quist, S.R., Gollnick, H.P., Natsuga, K., Aoyagi, S. & Watt, F.M. c-MYC-induced sebaceous gland differentiation is controlled by an androgen receptor/p53 axis. *Cell reports* **3**, 427-441 (2013).
11. Okabe, Y. & Medzhitov, R. Tissue-specific signals control reversible program of localization and functional polarization of macrophages. *Cell* **157**, 832-844 (2014).
12. Uribesalgo, I., Buschbeck, M., Gutierrez, A., Teichmann, S., Demajo, S., Kuebler, B., Nomdedeu, J.F., Martin-Caballero, J., Roma, G., Benitah, S.A. & Di Croce, L. E-box-independent regulation of transcription and differentiation by MYC. *Nature cell biology* **13**, 1443-1449 (2011).
13. Sada, A., Jacob, F., Leung, E., Wang, S., White, B.S., Shalloway, D. & Tumbar, T. Defining the cellular lineage hierarchy in the interfollicular epidermis of adult skin. *Nature cell biology* **18**, 619-631 (2016).

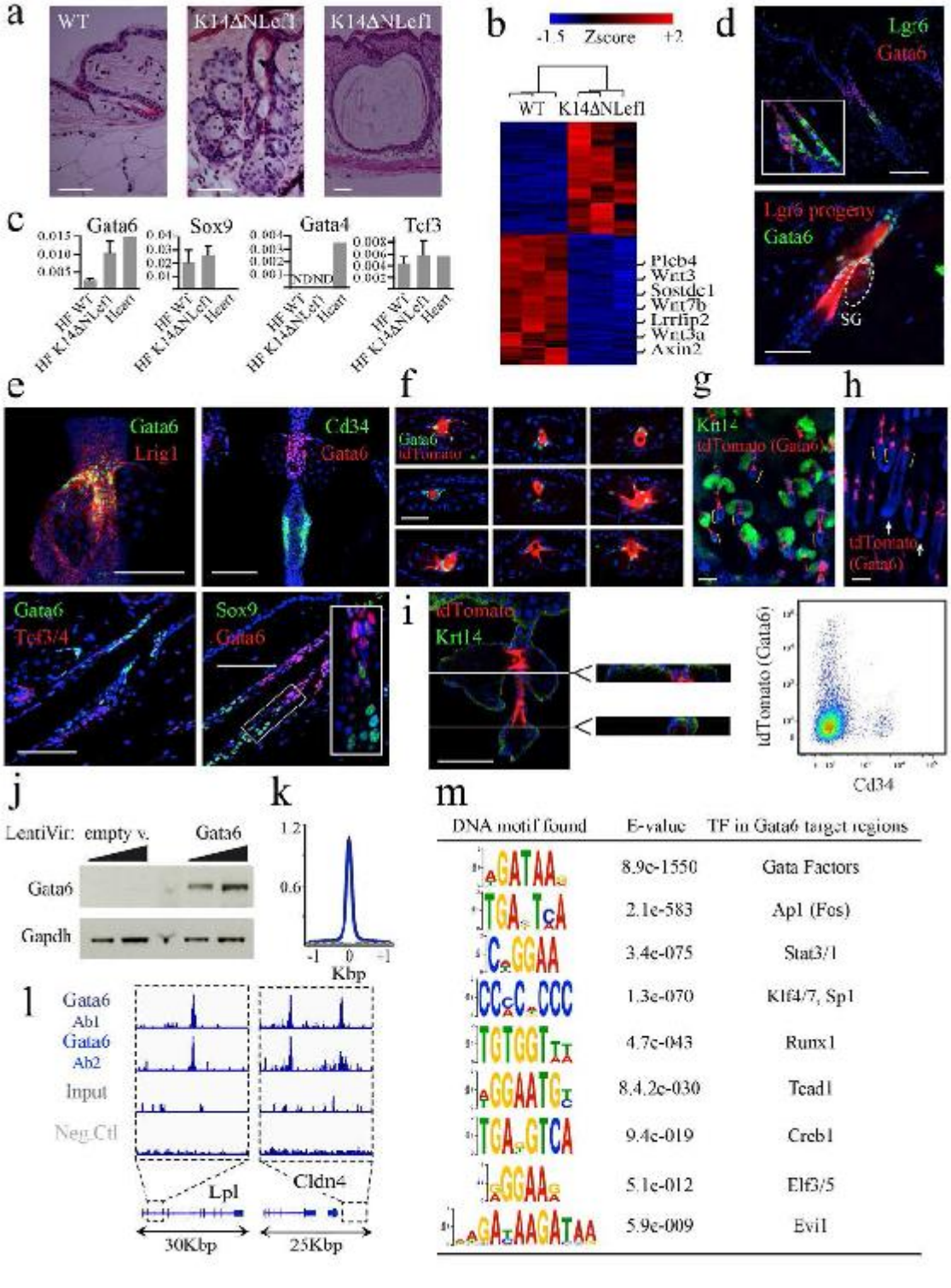

Supplementary Figure 1